

# The Weaknesses of Adversarial Camouflage in Overhead Imagery

Adam Van Etten

IQT Labs

avanetten@iqt.org

## Abstract

*Machine learning is increasingly critical for analysis of the ever-growing corpora of overhead imagery. Advanced computer vision object detection techniques have demonstrated great success in identifying objects of interest such as ships, automobiles, and aircraft from satellite and drone imagery. Yet relying on computer vision opens up significant vulnerabilities, namely, the susceptibility of object detection algorithms to adversarial attacks. In this paper we explore the efficacy and drawbacks of adversarial camouflage in an overhead imagery context. While a number of recent papers have demonstrated the ability to reliably fool deep learning classifiers and object detectors with adversarial patches, most of this work has been performed on relatively uniform datasets and only a single class of objects. In this work we utilize the VisDrone dataset, which has a large range of perspectives and object sizes. We explore four different object classes: bus, car, truck, van. We build a library of 24 adversarial patches to disguise these objects, and introduce a patch translucency variable to our patches. The translucency (or alpha value) of the patches is highly correlated to their efficacy. Further, we show that while adversarial patches may fool object detectors, the presence of such patches is often easily uncovered, with patches on average 24% more detectable than the objects the patches were meant to hide. This raises the question of whether such patches truly constitute camouflage. Source code is available at <https://github.com/IQTLabs/camolo>.*

## 1. Introduction

Computer vision algorithms are known to be susceptible to perturbations: A 2017 study summarized its findings like this: “Given a state-of-the-art deep neural network classifier, we show the existence of a universal (image-agnostic) and very small perturbation vector that causes natural images to be misclassified with high probability” [8]. Most recent research has focused on image classification and shown impressive results (e.g. [8], [3], [7], [4]) in inducing misclassifications. A smaller, though significant, body of work

has been performed on segmentation (e.g. [16], [8]).

There is also an increasing body of work around fooling advanced object detection systems. Some works ([14]) have shown an impressive ability to fool the YOLO [10] family of detectors with simulated autonomous vehicle data. Other works have concluded that at least for video object detection of vehicles, adversarial examples are not a significant concern due to varying distances and angles [9].

Of greatest relevance to this work are two recent papers that seek to fool YOLO. First up, [13] demonstrated the ability to fool YOLO models trained to detect people in surveillance cameras - significantly lowering the accuracy of person detectors trained on the Inria [2] dataset with the imposition of an adversarial patch. More recently, [1], adapted the codebase of [13] and demonstrated the ability to fool aircraft detectors with simulated patches trained on the DOTA dataset [15]. While these simulated patches of [1] may be quite effective in fooling aircraft detectors, they have not been tested in the real world or even projected in a realistic matter onto the objects of interest. Both papers used only single-class models and datasets with relatively little variability in object size and viewing perspective.

In Section 2 we detail what motivates why we seek to expand upon the above prior work. Section 3 details the drone imagery dataset used in this study, while Section 4 describes our algorithmic approach. In Section 5 we cover the results of our experiments, and in Section 6 we analyze the meaning of these results.

## 2. Motivation

There is much to explore in the adversarial camouflage space, but we will start with a simple mitigation example. In Section 1 we summarized prior work on effectively obfuscating objects with carefully designed patches. We ask a simple question: can the presence of adversarial patches be detected? To answer this question, we select a sampling of satellite image tiles (from the RarePlanes [12] dataset) and overlay a 10 existing performant adversarial patches on these image tiles (see Figure 1).

We overlay the ten patches of Figure 1 on 1667 image patches from the RarePlanes dataset, with 20% of these im-

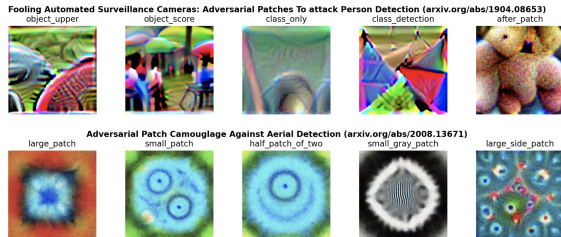


Figure 1. Legacy adversarial patches. Top: [13], bottom: [1].



Figure 2. Training data for our YOLV4 patch detection model.

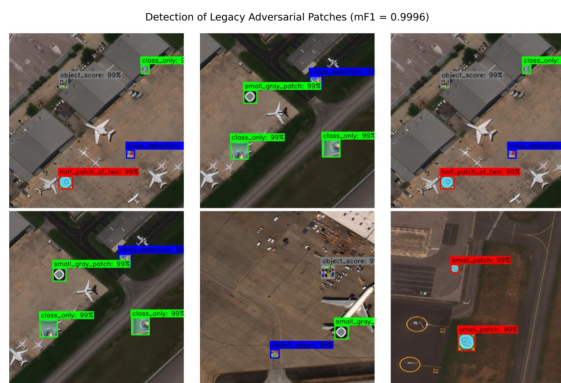


Figure 3. Detection of the presence of adversarial patches with our YOLV4 model.

ages reserved for validation. See Figure 2 for a sample of the training imagery. We train a 10-class YOLV4 model [5] (YOLV4 is built atop YOLO [10] and designed for overhead imagery analysis) for 20 epochs. We evaluate our trained model on a separate test set with 1029 images, and score with the F1 metric that penalizes both false positives and false negatives. The model yields an astonishing aggregate F1 = 0.999 for detection of the adversarial patches, with all 10 patches easily identified. We show a detection example in Figure 3.

If one can easily identify the existence of adversarial patches, the real-world effectiveness of these patches for camouflaging objects is called into question. One could simply run a patch detector in parallel with the original object detector. This motivates our study in Section 4 on whether “stealthy” patches can be designed that are both difficult to detect, and effective at obfuscating the presence of objects of interest.

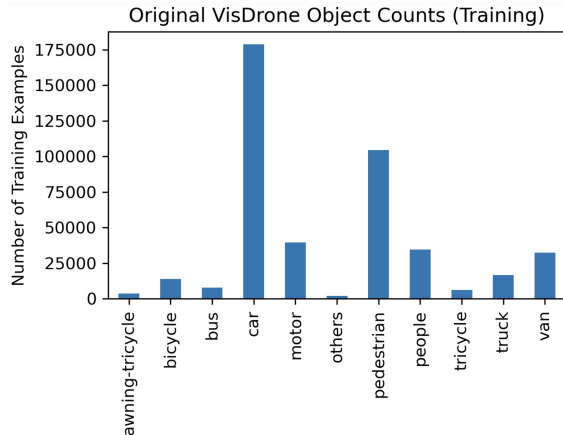


Figure 4. Object class counts for the raw VisDrone training dataset.

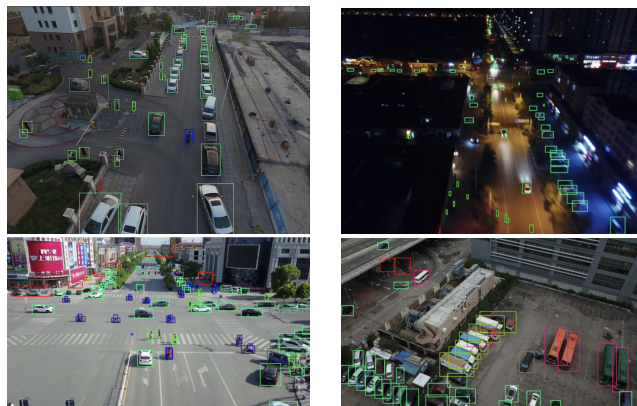


Figure 5. Sample images and ground truth bounding box labels for the raw VisDrone training dataset. Red boxes denote unlabeled regions.

### 3. VisDrone Dataset

For the remainder of this paper we use the VisDrone [17] dataset, specifically the object detection portion of VisDrone (VisDrone2019-DET). This dataset includes 6471 images taken from drones in the training set, with 1610 images in the test set. Bounding box annotations are provided for 11 object classes: pedestrian, person, car, van, bus, truck, motor, bicycle, awning-tricycle, tricycle and “others.” The dataset is highly imbalanced: “car” and “pedestrian” are by far the most common classes, see Figure 4, and a high number of labels per image (median of 43 labels per image, max of 914 labels). The altitude, viewing angle, and lighting conditions are highly variable, which complicates analysis of the imagery (see Figure 5). The 353,550 bounding box labels in the training set tend to be relatively small (median extent of 34 pixels), though the size is highly variable (std of 44 pixels), which is a due to the variance in altitude and viewing angle of the drone platform.

In this paper we focus on obfuscating vehicles, so we re-

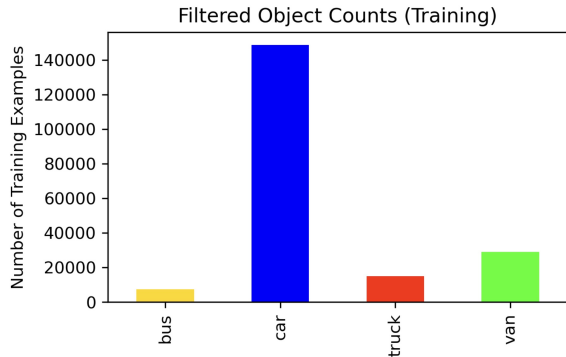


Figure 6. Object class counts for our filtered 4-class VisDrone training dataset.

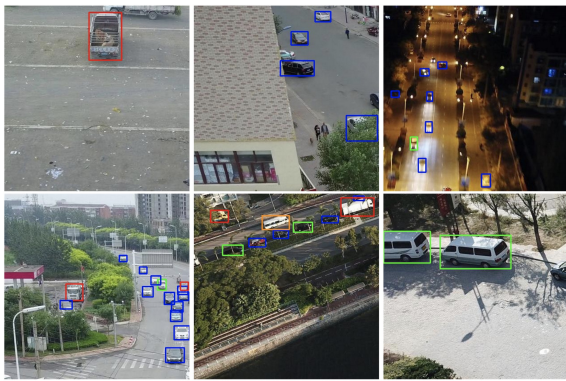


Figure 7. Training image chips for our 4-class model. Ground truth bounding box colors correspond to Figure 6.

tain only labels for four object classes (see Figure 6): bus, car, truck, and van. This filtering of labels simplifies both the object detection and camouflage tasks. We tile the VisDrone training imagery to  $416 \times 416$  pixel windows for ease of ingestion into the YOLO [11] object detection family, see Figure 7.

## 4. Adversarial Camouflage

### 4.1. Object Detector

We use the YOLTv4 [5] object detection framework to train a 4-class vehicle detector. We use a configuration file with an output feature map of  $26 \times 26$  for improved detection of small objects. We train for 80 epochs using stochastic gradient descent, with a learning rate of 0.001, and a momentum of 0.9. Predictions with the trained model are shown in Figure 8. We evaluate YOLT detection model performance with the 1610 images in the VisDrone test set, setting a true positive as a prediction of the correct class with an  $\text{IOU} \geq 0.5$ . Scores are shown in Table 1; we report  $1\sigma$  errors calculated via bootstrapping.

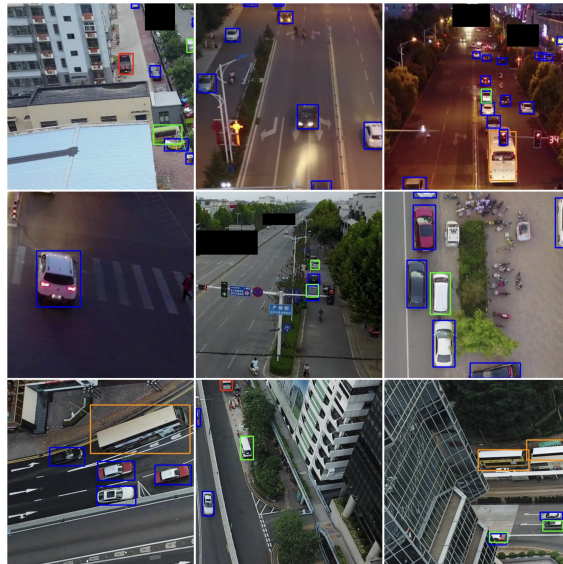


Figure 8. Predictions for the 4-class YOLT model (bus = yellow, car = blue, truck = red, van = green).

Table 1. YOLT 4-class Detection Performance

| Class | F1               |
|-------|------------------|
| Bus   | $0.59 \pm 0.06$  |
| Car   | $0.72 \pm 0.002$ |
| Truck | $0.43 \pm 0.009$ |
| Van   | $0.46 \pm 0.005$ |
| Mean  | $0.55 \pm 0.003$ |

### 4.2. Adversarial Patches

To train an adversarial patch, we develop the Camolo [6] codebase, which is a modification of the adversarial-yolo<sup>1</sup> codebase used in [13]. The adversarial-yolo codebase takes a trained model and labeled imagery as input, and attempts to create a patch that when overlaid on objects of interest will fool the detector. Camolo makes a number of modifications:

1. Increased flexibility with input variables (*e.g.* target patch size)
2. Use with more recent versions of YOLO
3. Allow patches to be semi-translucent

The most significant change (#3) is the method of overlaying patches according to a selected alpha value, which dictates how transparent the patch appears. We postulate that a semi-translucent patch may help camouflage the patches themselves. Previous studies have simply overwritten the existing pixels in an image with the desired patch. We combine the patch and original image pixels according

<sup>1</sup><https://gitlab.com/EAVISE/adversarial-yolo>





Figure 9. Sample adversarial patch from [13] overlaid (left = opaque, right = semi-transparent) on VisDrone imagery.

to a desired alpha value of the patch (alpha = 1 corresponds to an opaque patch, with alpha = 0 yielding an invisible patch). In Figure 9 we overlay a sample adversarial patch on VisDrone imagery with both the standard fully opaque method, as well as semi-transparent.

## 5. Experiments

### 5.1. Adversarial Patch Generation

We train a variety of adversarial patches using the Camolo codebase and VisDrone dataset. All experiments use the same initial dataset and model architecture. We vary the starting patch between experiments, trying both legacy patches as well as totally random starting points. Other variables are the allowed colors of the patches, and the alpha value (translucency) of the patches. The patch size (as a fraction of the area of the object of interest), and noise level is also varied. Finally, we select one of three losses for each experiment: object (focus only on minimizing bounding box detections), class (focus on confusing the class prediction of each bounding box), and object  $\times$  class. Training occurs for a minimum of 40 epochs for each experiment. Parameters are shown in Table 2. Most experiments aim to yield a non-detection (e.g. 1. obj\_only\_v0) though some experiments seek to confuse which object is classified (e.g. 3. class\_only\_v0), such as classifying a car as a truck. See Figure 10 for the trained patches.

In Figure 11 we show successful examples of patches fooling our trained object detector. Figure 12 shows how mF1 varies with alpha (translucency) and patch size. This plot shows the percentage reduction in vehicle detection provided by the patches; the Pearson correlation coefficient between vehicle detection mF1 reduction and size is 0.83 and the correlation coefficient between alpha and mF1 reduction is 0.76.

### 5.2. Detection of Patches

We showed in Figure 12 that our patches significantly reduce the ability of our trained YOLv4 model. In this section, we explore how easy it is to detect the existence

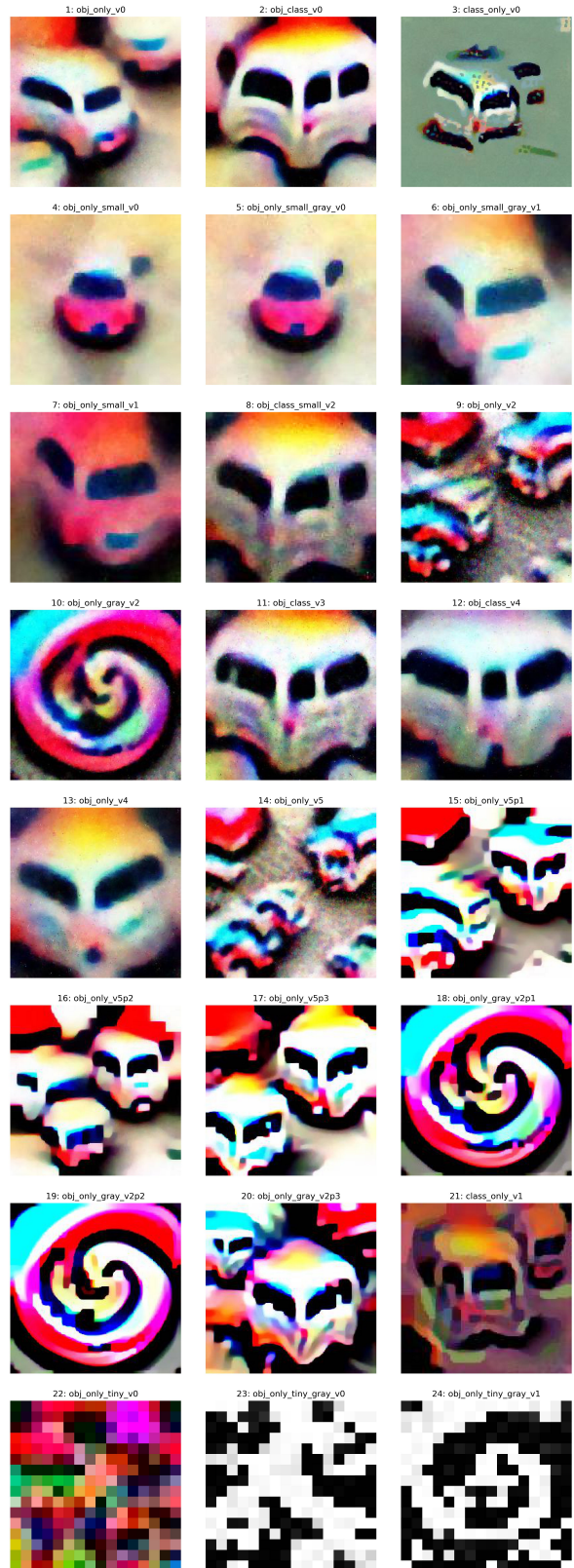


Figure 10. Trained adversarial patch library.



Table 2. Adversarial Patches Trained on VisDrone

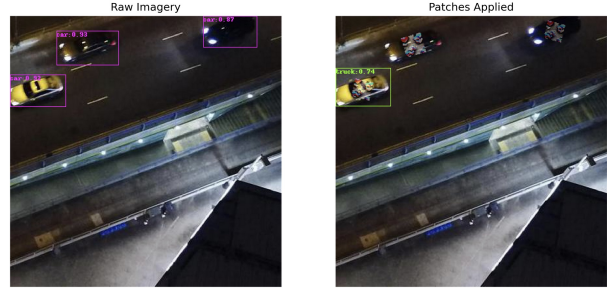
|    | Name                   | Loss      | Size | Alpha |
|----|------------------------|-----------|------|-------|
| 1  | obj_only_v0            | obj       | 0.2  | 0.4   |
| 2  | obj_class_v0           | obj * cls | 0.2  | 0.4   |
| 3  | class_only_v0          | cls       | 0.2  | 0.4   |
| 4  | obj_only_small_v0      | obj       | 0.2  | 0.3   |
| 5  | obj_only_small_gray_v0 | obj       | 0.2  | 0.3   |
| 6  | obj_only_small_gray_v1 | obj       | 0.16 | 0.4   |
| 7  | obj_only_small_v1      | obj       | 0.16 | 0.6   |
| 8  | obj_class_small_v2     | obj * cls | 0.16 | 0.75  |
| 9  | obj_only_v2            | obj       | 0.25 | 0.8   |
| 10 | obj_only_gray_v2       | obj       | 0.25 | 0.8   |
| 11 | obj_class_v3           | obj * cls | 0.16 | 0.6   |
| 12 | obj_class_v4           | obj * cls | 0.12 | 0.5   |
| 13 | obj_only_v4            | obj       | 0.12 | 0.5   |
| 14 | obj_only_v5            | obj       | 0.3  | 0.5   |
| 15 | obj_only_v5p1          | obj       | 0.25 | 0.5   |
| 16 | obj_only_v5p2          | obj       | 0.25 | 0.4   |
| 17 | obj_only_v5p3          | obj       | 0.2  | 0.4   |
| 18 | obj_only_gray_v2p1     | obj       | 0.25 | 0.7   |
| 19 | obj_only_gray_v2p2     | obj       | 0.25 | 0.6   |
| 20 | obj_only_gray_v2p3     | obj       | 0.2  | 0.7   |
| 21 | class_only_v1          | cls       | 0.25 | 0.9   |
| 22 | obj_only_tiny_v0       | obj       | 0.25 | 1.0   |
| 23 | obj_only_tiny_gray_v0  | obj       | 0.25 | 1.0   |
| 24 | obj_only_tiny_gray_v1  | obj       | 0.2  | 0.75  |

of these patches. Recall in the introduction that we found legacy patches to be detectable with nearly perfect performance. We train a generic patch detector using the same raw VisDrone imagery as in Section 5.1. We select 10 patches to train with, and overlay these patches on the training imagery. We train a YOLOv4 model, and test our generic patch detector by overlaying each of our 24 patches on the test set and scoring how robustly the patches can be detected. Performance is listed in Table 3, and illustrated in Figure 13. In Figure 13, the green line denotes the detection performance of the original 4-class model; the blue bars denote the performance of the 4-class detection model when the listed adversarial patch has been applied; the orange bars denote the detection performance of the model trained to detect the existence of patches. The 10 patches used to train the patch detection model are appended with an asterisk (*i.e.* \*) in Table 3 and 13.

## 6. Analysis

Note in Figure 13 that the orange bars are not significantly higher for asterisked (*i.e.* training) patches compared to the “unseen” patches. Also note that for most patches, it is easier to detect the existence of the patch than vehicles.

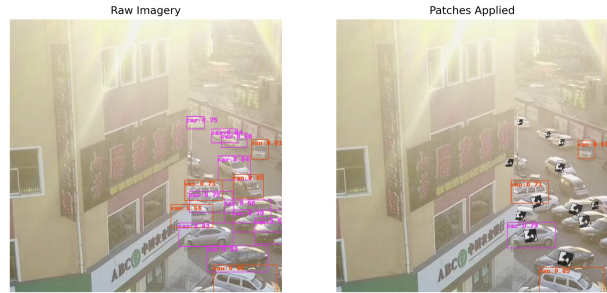
If we collapse the two performance of the two experiment groups (vehicle detection + patch detection), we are left with Figure 14, which shows a “detection” score: maximum of the two blue and orange bars in 13. This “de-



(a) 14. obj\_only\_v5



(b) 21. class\_only\_v1



(c) 24. obj\_only\_tiny\_gray\_v1

Figure 11. Detection of vehicles with the original trained model with raw test imagery (left) and patches applied on cars (right).

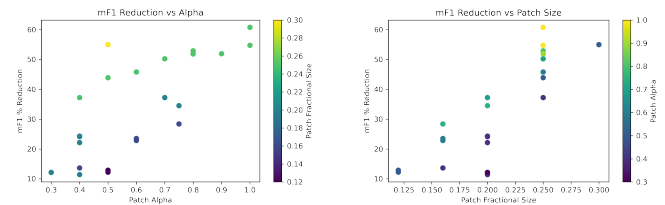


Figure 12. Patch performance as a function of size and alpha (higher is better).

tection” score provides a measure of the efficacy of the patch, since an easily detected patch is not terribly effective at camouflage, since the patch itself exposes the presence of the object of interest. Recall that in Figures 13 and 14, lower is better. Note also that most patches provide no aggregate benefit. Yet the two black and white patches (obj\_only\_tiny\_gray\_v0 and obj\_only\_tiny\_gray\_v1) are the most effective. The precise reason for this efficacy will be left to later work, but we postulate that the marked differ-

Table 3. Detection Performance of Various Models

|    | Model Name             | mF1 <sub>camo</sub> | F1 <sub>patch</sub> |
|----|------------------------|---------------------|---------------------|
| 1  | obj_only_v0*           | 0.44                | 0.77                |
| 2  | obj_class_v0*          | 0.43                | 0.76                |
| 3  | obj_only_small_v0*     | 0.49                | 0.70                |
| 4  | obj_only_small_v1*     | 0.44                | 0.69                |
| 5  | obj_class_v3*          | 0.43                | 0.70                |
| 6  | obj_only_v4*           | 0.49                | 0.55                |
| 7  | obj_only_v5*           | 0.28                | 0.86                |
| 8  | obj_only_v5p3*         | 0.43                | 0.75                |
| 9  | obj_only_gray_v2p2*    | 0.32                | 0.87                |
| 10 | obj_only_gray_v2p3*    | 0.36                | 0.82                |
| 11 | class_only_v0          | 0.49                | 0.42                |
| 12 | obj_only_small_gray_v0 | 0.49                | 0.69                |
| 13 | obj_only_small_gray_v1 | 0.48                | 0.61                |
| 14 | obj_class_small_v2     | 0.41                | 0.70                |
| 15 | obj_only_v2            | 0.29                | 0.87                |
| 16 | obj_only_gray_v2       | 0.29                | 0.89                |
| 17 | obj_class_v4           | 0.49                | 0.44                |
| 18 | obj_only_v5p1          | 0.33                | 0.83                |
| 19 | obj_only_v5p2          | 0.36                | 0.79                |
| 20 | obj_only_gray_v2p1     | 0.30                | 0.89                |
| 21 | class_only_v1          | 0.29                | 0.79                |
| 22 | obj_only_tiny_v0       | 0.28                | 0.80                |
| 23 | obj_only_tiny_gray_v0  | <b>0.25</b>         | 0.13                |
| 24 | obj_only_tiny_gray_v1  | 0.38                | <b>0.12</b>         |
|    | mean                   | 0.38                | 0.68                |

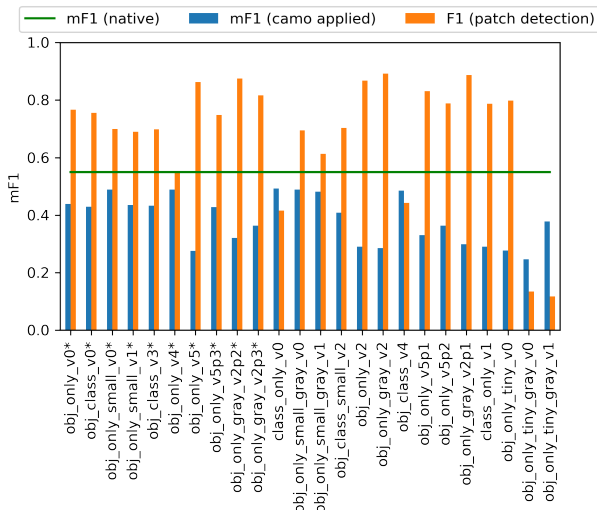


Figure 13. Detection performance for each model.

ence of these two patches (*i.e.* grayscale vs color) from the ten patches in our patch detector training set is largely responsible.

Figure 15 shows how aggregate varies with alpha and patch size. Recall from Figure 12 that larger and more opaque (higher alpha) patches are more effective at confusing the vehicle detector. Yet Figure 15 shows that patches

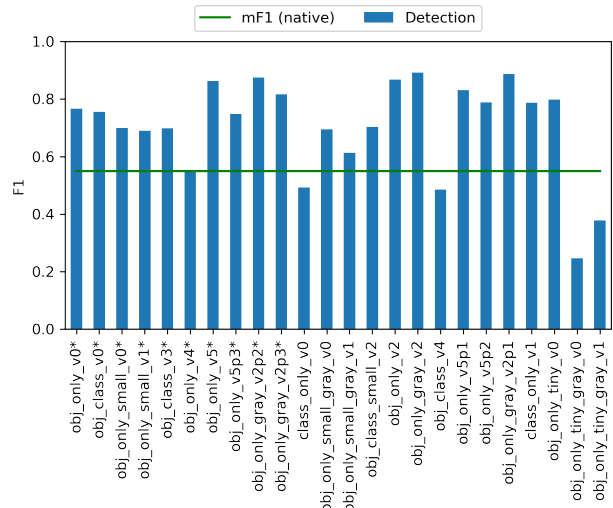


Figure 14. Aggregate detection performance for each model. The lower the value, the more effective the patch.

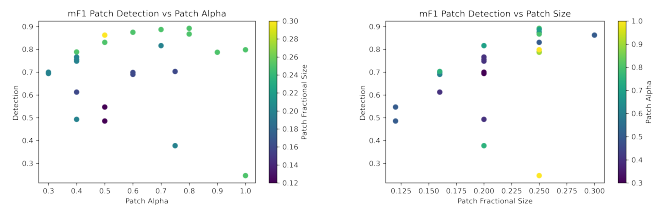


Figure 15. Detection dependence on size, alpha (lower is better).

with higher alpha and larger sizes are actually less effective in aggregate performance since the existence of large, opaque patches is far easier to detect. In fact, in terms of aggregate performance, smaller, more translucent patches are preferred (Pearson correlation between detection and alpha: -0.76, Pearson correlation between detection and patch size: -0.83). Ultimately, for true camouflage, one should apparently prioritize patch stealthiness.

## 7. Conclusions

Adversarial patches have been shown to be effective in camouflaging objects in relatively homogeneous datasets such as Inria and DOTA. In this paper we showed that while legacy patches may be effective in hiding people and aircraft, such patches are trivial to detect. This motivates our study of whether “stealthy” patches can be designed to obfuscate objects in overhead imagery. Using the diverse Vis-Drone dataset we train a library of 24 adversarial patches with various input parameters. While most of these patches significantly reduce the detection of our objects of interest (buses, cars, trucks, vans), most patches are still easier to detect than vehicles. Our two black-and-white patches are

poorly detected with our patch detection model, however, due to their significant variance from the patch training set. This raises the question: how large and diverse of a patch library is required to be truly effective? And how much effort is required on the mitigation side in order to train a robust patch detection model that will effectively combat adversarial camouflage? We have provided some first hints to these questions, but much work remains to be done. Besides diving into these questions, in future work we hope to introduce false positives into imagery (*e.g.* can a simple pattern laid out in an empty field trick a computer vision model into “detecting” a full parking lot).

## References

- [1] Ajaya Adhikari, Richard J. M. den Hollander, Ioannis Tolios, Michael van Bekkum, Anneloes Bal, Stijn Hendriks, Maarten Kruithof, Dennis Gross, Nils Jansen, Guillermo A. Pérez, Kit Buurman, and Stephan Raaijmakers. Adversarial patch camouflage against aerial detection. *CoRR*, abs/2008.13671, 2020.
- [2] N. Dalal and B. Triggs. Histograms of oriented gradients for human detection. In *2005 IEEE Computer Society Conference on Computer Vision and Pattern Recognition (CVPR’05)*, volume 1, pages 886–893 vol. 1, 2005.
- [3] Ranjie Duan, Xingjun Ma, Yisen Wang, James Bailey, A. Kai Qin, and Yun Yang. Adversarial camouflage: Hiding physical-world attacks with natural styles. *CoRR*, abs/2003.08757, 2020.
- [4] Ranjie Duan, Xiaofeng Mao, A. Kai Qin, Yun Yang, Yuefeng Chen, Shaokai Ye, and Yuan He. Adversarial laser beam: Effective physical-world attack to dnns in a blink. *CoRR*, abs/2103.06504, 2021.
- [5] Adam Van Etten. Announcing yoltv4: Improved satellite imagery object detection. <https://medium.com/@avanetten>, 2021.
- [6] Adam Van Etten. Camolo. <https://github.com/IQTLabs/camolo>, 2022.
- [7] Ivan Evtimov, Kevin Eykholt, Earlence Fernandes, Tadayoshi Kohno, Bo Li, Atul Prakash, Amir Rahmati, and Dawn Song. Robust physical-world attacks on machine learning models. *CoRR*, abs/1707.08945, 2017.
- [8] Jan Hendrik Metzen, Mummadi Chaithanya Kumar, Thomas Brox, and Volker Fischer. Universal Adversarial Perturbations Against Semantic Image Segmentation. *arXiv e-prints*, page arXiv:1704.05712, Apr. 2017.
- [9] Jiajun Lu, Hussein Sibai, Evan Fabry, and David A. Forsyth. NO need to worry about adversarial examples in object detection in autonomous vehicles. *CoRR*, abs/1707.03501, 2017.
- [10] Joseph Redmon, Santosh Kumar Divvala, Ross B. Girshick, and Ali Farhadi. You only look once: Unified, real-time object detection. *CoRR*, abs/1506.02640, 2015.
- [11] Joseph Redmon and Ali Farhadi. Yolov3: An incremental improvement. *arXiv*, 2018.
- [12] Jacob Shermeyer, Thomas Hossler, Adam Van Etten, Daniel Hogan, Ryan Lewis, and Daeil Kim. Rareplanes: Synthetic data takes flight. *CoRR*, abs/2006.02963, 2020.
- [13] Simen Thys, Wiebe Van Ranst, and Toon Goedemé. Fooling automated surveillance cameras: adversarial patches to attack person detection. *CoRR*, abs/1904.08653, 2019.
- [14] Jiakai Wang, Aishan Liu, Zixin Yin, Shunchang Liu, Shiyu Tang, and Xianglong Liu. Dual attention suppression attack: Generate adversarial camouflage in physical world. *CoRR*, abs/2103.01050, 2021.
- [15] Gui-Song Xia, Xiang Bai, Jian Ding, Zhen Zhu, Serge J. Belongie, Jiebo Luo, Mihai Datcu, Marcello Pelillo, and Liangpei Zhang. DOTA: A large-scale dataset for object detection in aerial images. *CoRR*, abs/1711.10398, 2017.
- [16] Cihang Xie, Jianyu Wang, Zhishuai Zhang, Yuyin Zhou, Lingxi Xie, and Alan L. Yuille. Adversarial examples for semantic segmentation and object detection. *CoRR*, abs/1703.08603, 2017.
- [17] Pengfei Zhu, Longyin Wen, Dawei Du, Xiao Bian, Heng Fan, Qinghua Hu, and Haibin Ling. Detection and tracking meet drones challenge. *IEEE Transactions on Pattern Analysis and Machine Intelligence*, pages 1–1, 2021.